

WELDING OF THE STEEL GRADE S890QL

VARJENJE JEKLA KVALITETE S890QL

Roman Celin¹, Jure Bernetič², Danijela Anica Skobir Balantič¹

¹Institute of Metals and Technology, Lepi pot 11, 1000 Ljubljana, Slovenia

²Acroni, d. o. o., Cesta Borisa Kidriča 44, 4270 Jesenice, Slovenia

roman.celin@imt.si

Prejem rokopisa – received: 2014-07-15; sprejem za objavo – accepted for publication: 2014-07-25

Quenched and tempered high-strength steels are widely used in the construction of steel structures. However, because of their properties, care must be taken in order to determine suitable welding parameters. One way is to use the weld-heat-flow theory with the use of the weld-bead cooling time $t_{8/5}$ and the recommendations of the standard EN 1011-2. The chosen weld parent material was high-strength S890QL steel with the filler welding wire G Mn4Ni1.5CrMo, which were used to produce a sound butt weld. Mechanical testing and a metallographic examination of the weld samples were carried out. The tensile test showed undermatching of the weld joint, with a satisfactory Charpy V notch toughness. The metallographic investigation revealed a microstructure variation in different areas of the weld joint. The highest values of the hardness HV10 were measured in the heat-affected zone.

Keywords: welding, high-strength steel, cooling time $t_{8/5}$, microstructure, mechanical testing

Poboljšana visokotrдна jekla se vsestransko uporabljajo pri gradnji jeklenih konstrukcij. Zaradi njihovih lastnosti je potrebna pazljivost pri določanju parametrov varjenja. Eden od načinov določitve parametrov varjenja je z uporabo teorije prenosa toplote in časa ohlajanja varka $t_{8/5}$ z upoštevanjem navodil, podanih v standardu EN 1011-2. Za izvedbo sočelnega zavarjenega spoja sta bila izbrana visokotrдно poboljšano jeklo z oznako S890QL in dodajni material varilna žica z oznako G Mn4Ni1,5CrMo. Pri vzorcih zavarjenega spoja so bile izvedene mehanske in metalografske preiskave. Z nateznimi preizkusi je bila ugotovljena trdnostna neenakost z ustrežno vrednostjo V udarne žilavosti po Charpyju. Z metalografskimi preiskavami so bile odkrite spremembe v mikrostrukturi na različnih področjih zavarjenega spoja. Maksimalna trdota HV10 je bila izmerjena v toplotno vplivanem področju zavarjenega spoja.

Ključne besede: varjenje, visokotrдно jeklo, čas ohlajanja $t_{8/5}$, mikrostruktura, mehanske preiskave

1 INTRODUCTION

Developments in steel making, rolling and heat treatment have resulted in high-strength steels¹. The EN 10025 standard² contains a wide variety of steel grades. One such steel-grade designation is S890QL quenched and tempered structural steel with a minimum yield strength of 890 MPa.

In the process of high-strength steel component manufacturing, one must be careful with the selection of the welding parameters, the welding current I , the welding arc voltage U , the welding speed v , the cooling time $t_{8/5}$, and the specific heat input. These are the most influential factors with respect to the quality of the weld joint, besides the base and the filler material, the weld geometry, the welding equipment and a skilled welder. A low heat input, for instance, affects the increase in the strength and hardness of a welded joint with possible cold cracking. On the other hand, a high heat input might cause the formation of a coarse-grained microstructure with a reduced strength of the weld joint³.

One way to approach the determination of the welding parameters is to use the theory of weld heat flow⁴⁻⁸.

In the course of our work the empirical equations derived from the theory of weld heat flow were used. During the welding process almost all the energy is concentrated in a very small volume beneath the arc in the weld melt⁹ and has an influence on the solidification and

cooling time. The cooling time $t_{8/5}$ is the time needed for a weld pass and its heat-affected zone to cool from the temperature of 800 °C to 500 °C (**Figure 1**) and has an influence on the microstructure of the weld joint. It can also be used for checking the effect of the reheat on the microstructure obtained during the primary cooling¹⁰. In the temperature range between 800 °C and 500 °C a microstructure transformation occurs, and depending on the $t_{8/5}$, a ferritic, perlitic, bainitic and martensitic microstructure can form. With a prolonged $t_{8/5}$ it is possible that only ferrite and perlite form from the austenite.

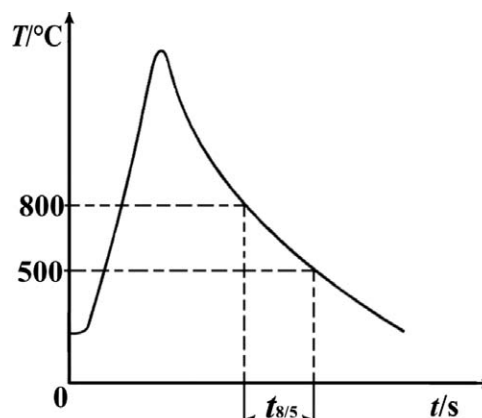


Figure 1: Temperature cycle and cooling time $t_{8/5}$

Slika 1: Potek temperature in čas ohlajanja $t_{8/5}$

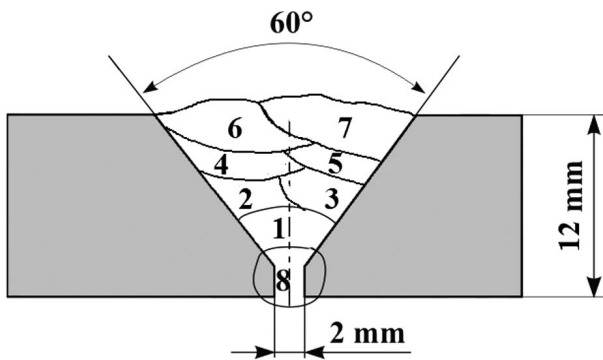


Figure 2: Sketch of the welded joint
Slika 2: Skica zavarjenega spoja

This paper presents an investigation of a commercial grade Micral 890 high-strength steel weld joint with:

- plate thickness d of a 12 mm,
- V-shaped joint geometry (Figure 2),
- MAG welding procedure with a shielding gas mixture (82 % Ar + 18 % CO₂) in a flat position,
- welding wire filler material of $\phi = 1.2$ mm with the EN 12534 designation G Mn4Ni1.5CrMo with undermaching properties ($R_{p0.2} = 720$ MPa and $R_m = 780$ MPa catalogue data).

The chemical composition of the used Micral 890 MPa plate is shown in Table 1.

Table 1: Chemical composition of steel in mass fractions, w/%
Tabela 1: Kemijska sestava jekla v masnih deležih, w/%

C	Si	Mn	P	S	Cr	Ni	Cu
0.17	0.30	1.31	0.010	0.001	0.46	0.12	0.21
Mo	V	Ti	Nb	Al	B	N	-
0.288	0.01	0.014	0.022	0.057	0.0029	0.0066	-

The main goal of the investigation was to produce a weld joint with as low a heat input and as short a $t_{8/5}$ as possible and without weld defects. The welding parameters were determined using the theory of weld heat flow and the recommendations given in^{11,12}.

2 WELDING PARAMETERS

The recommendations written in^{10,11} were taken into consideration and empirical equations for the calculation of the cooling time were applied. The effect of the alloying elements on the carbon equivalent (C_{ET}) is given by Equation (1):

$$C_{ET} = C + \frac{Mn+Mo}{10} + \frac{Cr+Cu}{20} + \frac{Ni}{40} = 0.365 \% \quad (1)$$

The calculation of the preheat temperature T_P is:

$$T_P = 697 \cdot C_{ET} + 160 \cdot \tanh\left(\frac{d}{35}\right) + 62 \cdot HD^{0.35} + (53 \cdot C_{ET} - 32) \cdot Q - 328 = 75.3 \text{ }^\circ\text{C} \quad (2)$$

where HD is a conservatively estimated hydrogen content of 5 mL on 100 g of weld metal for the welding method¹¹. A linear heat input E of 0.8 kJ/mm was chosen for the initial calculation:

$$Q = \eta \cdot E = 0.68 \text{ kJ/mm} \quad (3)$$

where η is the arc thermal efficiency of 0.85 for the MAG welding procedure¹¹.

A decision was made to preheat the weld seam area material to $T_P = 130$ °C. Using the heat-flow theory one must assume that for a given combination of material thickness, heat input and preheat temperature, the heat flow might have two- or three-dimensional features, so a calculation of the transition thickness d_t is necessary (Eq. 4):

$$d_t = \sqrt{\frac{\eta \cdot E}{2 \cdot \rho \cdot c} \cdot \left(\frac{1}{500 - T_0} + \frac{1}{800 - T_0} \right)} = 0.013 \text{ m} \quad (4)$$

where ρ is the steel density of 7850 kg/m³, c is the metal heat capacity of 0.994 kJ/(kg K), and $T_0 = T_P = 130$ °C. The plate thickness $d = 12$ mm is less than the transitional thickness $d_t = 13$ mm. In this case the equation for two-dimensional heat flow is applicable for the $t_{8/5}$ calculation:

$$t_{8/5} = (4300 - 4.3) \cdot 10^5 \cdot \frac{Q^2}{d^2} \cdot \left\{ \left(\frac{1}{500 - T_0} \right)^2 - \left(\frac{1}{800 - T_0} \right)^2 \right\} \cdot F_2 = 7 \text{ s} \quad (5)$$

where F_2 is the shape factor of 0.9 for two-dimensional heat flow¹¹. From the calculated data, a relationship between the particular plate thickness and the heat input for a given T_P and $t_{8/5}$ is shown in Figure 3.

Also, the relationship between the transition thickness and the heat input is presented in Figure 4, where the transition thickness increases with increasing heat input. Equation 4 can be written as a product of the voltage and the welding current divided by the welding speed v /(mm/s):

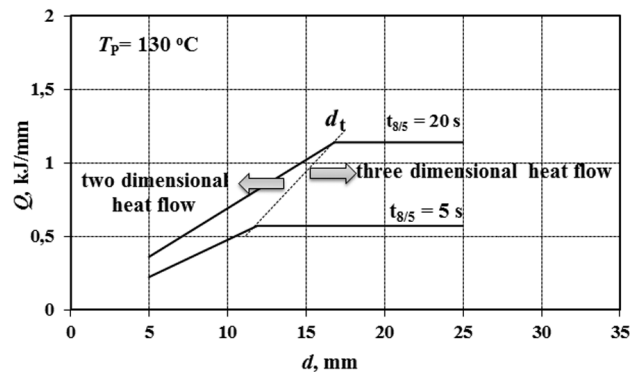


Figure 3: Relationship between the heat input, the transition thickness d_t and the plate thickness for a given T_P

Slika 3: Razmerje med vnosom toplote, prehodno debelino d_t in debelino pločevine pri dani T_P

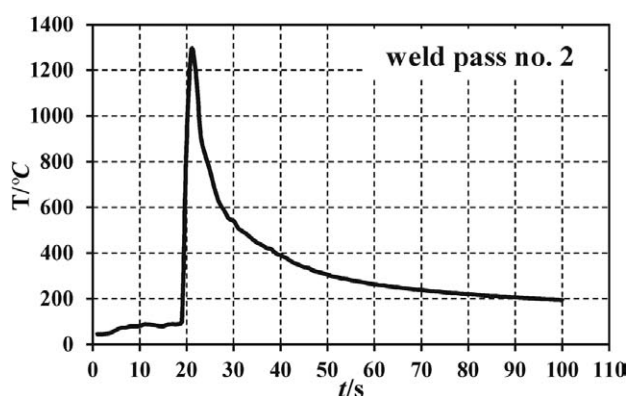


Figure 4: Weld pass no. 2 – temperature cycle

Slika 4: Polnilni varek št. 2 – potek temperature

$$Q = \eta \cdot E = \eta \cdot \frac{U \cdot I}{v \cdot 1000} \text{ kJ/mm} \quad (6)$$

By combining the data from **Figure 4** and the relationships in Equation 7, a range of welding parameters was determined $U = 22\text{--}30$ V, $I = 220\text{--}250$ A and $v = 5\text{--}8$ mm/s, with a heat input of $0.51\text{--}1.275$ kJ/mm.

3 EXPERIMENTAL

Prior to any activity a quantitative chemical analysis of the Micral 890 plate sample with an ICP mass spectrometer was made. The results of the chemical analysis were used in a pre-heat temperature calculation. The edges of two plates, each 700 mm long and 150 mm wide, were machined in a V-shaped butt joint (**Figure 1**). A skilled welder then manually welded the testing plate with eight passes (**Figure 2**) using a MAG welding procedure in a flat (PA) position, using a $\phi = 1.2$ mm under-match welding wire G Mn4Ni1.5CrMo (EN ISO 16834:2012 Classification).

The welding current, voltage and time were registered during the procedure. The cooling time $t_{8/5}$ was measured in two weld passes (No. 2 and No. 4) by dipping a Ni-CrNi thermocouple directly into a molten weld bead. The temperature sampling rate was one reading per second with all the readings stored in an instrument memory card¹³. The temperature T_P between the

Table 2: Recorded and calculated welding parameters

Tabela 2: Ugotovljeni in izračunani varilni parametri

pass no.	l mm	t s	I A	U V	T_P °C	v^a mm/s	Q^a kJ/mm
1	610	94	165	20.4	130	6.49	0.46
2	610	76	230	24.5	150	8.02	0.63
3	670	80	220	24.5	150	8.37	0.57
4	670	80	228	24.5	160	8.37	0.60
5	670	98	237	24.5	160	6.83	0.76
6	670	98	230	23.5	170	6.83	0.71
7	670	97	235	23.5	170	6.90	0.72
8	660	113	215	22	130	5.84	0.73

Note: ^a calculated values

weld passes varied from 130 °C to 170 °C. After welding, a surface (visual and liquid penetrant) and volumetric (X-ray) non-destructive testing was performed with subsequent machining of the standard specimens, which were tested as follows:

- 3 flat specimens for the tensile test at room temperature,
- 18 specimens for the Charpy V-notch toughness tests at -20 °C and -40 °C using an impact pendulum with a capacity 300 J,
- 1 specimen for the HV10 hardness testing and a metallographic investigation.

4 RESULTS AND DISCUSSION

4.1 Welding

The recorded average welding parameters and the calculated welding speed and heat input are given in **Table 2**. The data in **Table 2** shows that the low heat input during the welding of subsequent passes was $0.46\text{--}0.73$ kJ/mm, which is on the lower side of the predicted heat input range.

After temperature-data acquisition from the memory card and a data analysis for the welding pass no. 2 and no. 4, the cooling times $t_{8/5}$ of 8 s and 7 s, respectively, were determined. **Figure 4** shows the weld pass no. 2 temperature cycle. A similar temperature cycle was recorded during weld pass no. 4 cooling.

With applying Eq. 6 and the data in **Table 2** the theoretical values $t_{8/5}$ of 6.2 s and 6.6 s for weld pass no. 2 and pass no. 4, respectively, were calculated. We must assume that the equations for the cooling time (Eq. 6) might not be completely fulfilled, and thus the calculated values vary from the measured ones.

4.2 Mechanical testing

Prior to the machining of the standard test specimens for mechanical testing, a non-destructive examination of the welded joint was performed. A visual and liquid-penetrant inspection did not reveal any surface-flaw indications. Also, the X-ray inspection did not discover any flaws in the weld joint. A flat specimen tensile test was performed according to SIST EN ISO 4136:2011. The tensile test results are given in **Table 3**.

Table 3: Tensile test results

Tabela 3: Rezultati nateznih preizkusov

no.	yield stress	tensile strength	break
	$R_{p0.2}$ /MPa	R_m /MPa	
1	798	934	HAZ
2	811	928	WM
3	849	932	WM

The values of the yield stress and the tensile strength of the weld joint flat specimens is above the value of the filler wire of 780 MPa.

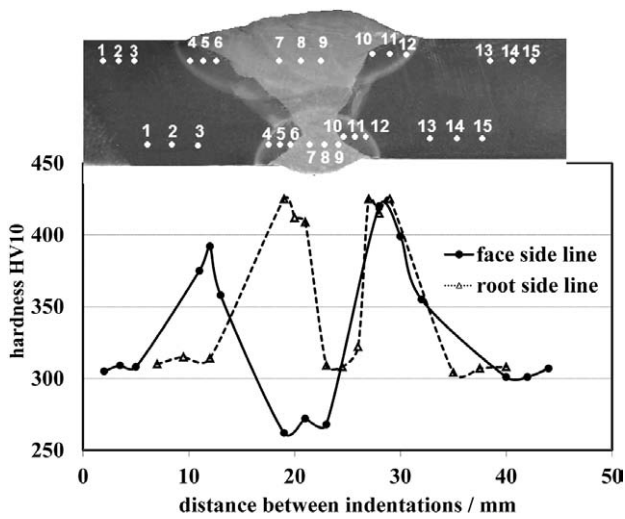


Figure 5: Hardness HV10 distribution through weld macro-section
Slika 5: Potek trdot HV10 na makroobrusu zavarjenega spoja

The Charpy impact tests were performed at $-20\text{ }^{\circ}\text{C}$ and $-40\text{ }^{\circ}\text{C}$ on a testing machine with an impact pendulum of capacity 300 J. Altogether, eighteen samples were machined with a V-notch position in the parent metal, the heat-affected zone and the weld metal. For all the specimens the pendulum-absorbed energy was higher than 27 J at $-40\text{ }^{\circ}\text{C}$, which is the delivery condition².

Table 4 shows the Charpy impact test results from which we can conclude that all the V notches in the WM and HAZ samples were machined in an area that was tempered by a subsequent pass heat input. Also, the use of the undermatch filler material contributed to satisfactory Charpy impact test results.

The hardness testing HV10 across the weld joint, from the parent material through the heat-affected zone

Table 4: Charpy impact tests results

Tabela 4: Rezultati preizkusa Charpyjeve udarne žilavosti

V notch position	$T/^{\circ}\text{C}$	absorbed energy, E_{abs}/J
parent material PM	-20	111, 129, 82
	-40	55, 75, 56
heat affected zone HAZ	-20	74, 66, 72
	-40	54, 61, 60
weld metal WM	-20	79, 77, 71
	-40	54, 56, 74

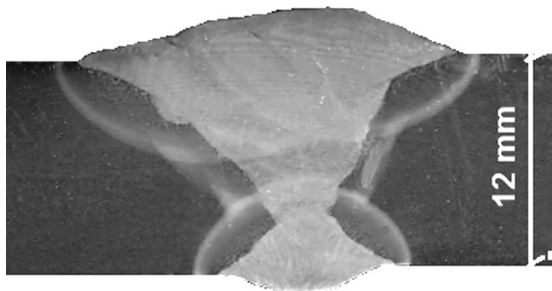


Figure 6: Welded joint macro-section
Slika 6: Makroposnetek zavarjenega spoja

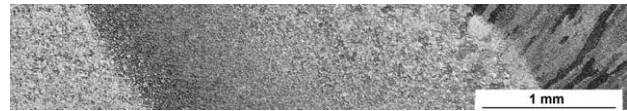


Figure 7: Transition from parent material to weld metal
Slika 7: Prehod iz osnovnega materiala v zvar

and the weld metal, to the same areas on the other side of the joint was performed. Figure 5 shows two lines of hardness-test indentations, 2 mm from the top side and 2 mm from the root side of the weld, with corresponding results in a graph.

The results of the hardness testing show how much the material microstructure has been changed by the heat input of the multipass welding. The maximum hardness HV10 was measured at indentations no. 4, 5, 6 and 10, 11, 12 of the root side and the top side. These HV10 values are placed on the un-tempered area of the heat-affected zone, and hence the values are higher.

4.3 Metallographic investigation

The microstructure of the welded joint specimen was evaluated using a light microscope (LM) and a scanning electron microscope (SEM). Figure 6 shows the etched welded-joint macro-section with a visible reheat thermal cycle for each weld pass. The area of normalized and refined microstructure, due to the effect of the subsequent pass on the weld metal of the previous pass, can be distinguished¹⁴ (Figure 6).

Figure 7 shows the root side longitudinal microstructure transition from the parent material (PM) through the heat-affected zone (HAZ) to the weld metal (WM). The PM has a tempered martensitic microstructure. In the HAZ fine-grain zone, the coarse-grain zone with a fusion line on the WM boundary is visible. The fine-grain zone has a martensitic microstructure with individual bainite grains (Figure 8). The coarse-grain zone on the border with the WM has a martensitic microstructure (Figure 9) with larger grains due to the overheating during the

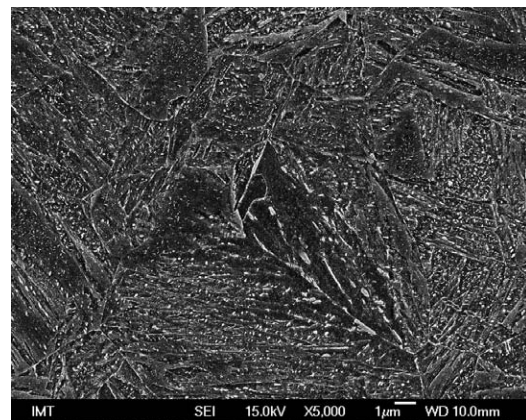


Figure 8: Fine-grained HAZ – martensite bainite microstructure
Slika 8: Toplotno vplivano področje drobnih zrn – martenzitno-bainitna mikrostruktura

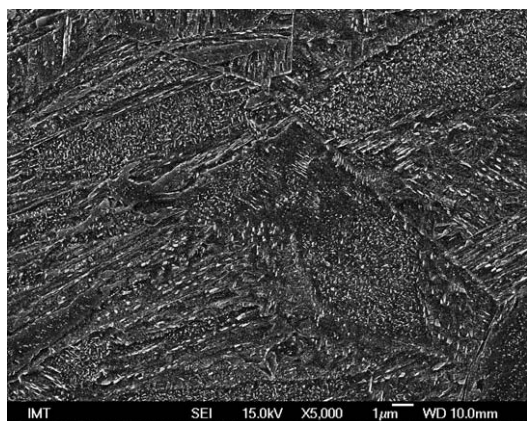


Figure 9: Coarse-grained HAZ – martensite microstructure

Slika 9: Toplotno vplivano področje grobih zrn – martenzitna mikrostruktura

welding. The fusion line between the weld metal and the HAZ is visible with the WM dendrite bainite microstructure (**Figure 10**).

5 CONCLUSIONS

This paper presents a determination of the welding parameters for a S890QL high-strength steel using empirical equations derived from the weld-heat-flow theory. The goal was to produce a weld joint without any defects, with a low heat input and as short a $t_{8/5}$ as possible. Based on the investigation the following conclusions can be drawn:

- It is possible to use empirical equations for a determination of the quenched and tempered high-strength welding parameters.
- The HV10 hardness-measurement results showed that the subsequent weld pass tempered the previous weld metal, thus reducing the hardness.
- The measured Charpy impact toughness that absorbed the impact energy of the weld specimen was higher than the S890QL delivery requirements.
- The cold cracking of the weld joint was avoided with the use of a sufficiently high pre-heat temperature and an undermatching filler material (welding wire).
- It is a general recommendation that the pass sequence should be such that there is no contact between the last cap pass and the parent metal. In our case this recommendation was not fulfilled, and therefore the highest HV10 values are in the HAZ.
- There is a poor deformability of the local HAZ area as a consequence of the high HV10 values.

NOTE

The selection of the welding parameters described in this article is not definitive. Welding joints can be pro-

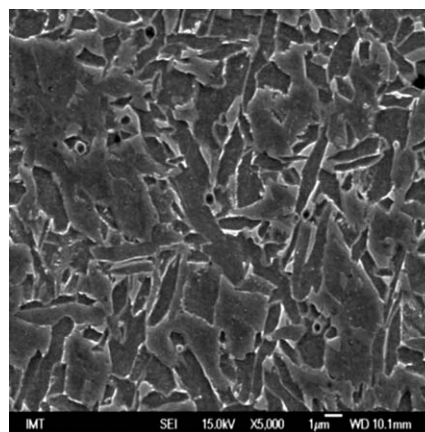


Figure 10: Weld metal bainite microstructure

Slika 10: Bainitna mikrostruktura vara

duced with more suitable welding parameters or processes. Therefore, a welding-procedure qualification test in accordance with steel manufacturer's recommendations and an appropriate standard must be carried out.

Acknowledgment

This article presents work that has been done with technical support of Acroni, d. o. o., Jesenice, Slovenia.

6 REFERENCES

- ¹ P. Collin, M. Möller, M. Nilsson, S. Törnblom, Undermatching Butt welds in high strength steel, IABSE Symposium, Bangkok, 2009, 96–106
- ² SIST EN 10025-6: 2005+A1: 2009, Hot rolled products of structural steels – Part 6: Technical delivery conditions for flat products of high yield strength structural steels in the quenched and tempered condition, 2006, 2009
- ³ V. Grdun, B. Godec, Mater. Tehnol., 36 (2002) 5, 247–254
- ⁴ N. Rykalin, Calculation of Heat Flow in Welding, Document 212-350-74, International Institute of Welding, London, 1974
- ⁵ R. Pavelic, R. Tanakuchi, O. Czehara, P. Myers, Welding Journal, 48 (1969) 7, 295
- ⁶ D. Rosenthal, R. Schmerber, Welding Journal, 17 (1983) 4, 2
- ⁷ I. S. Kim, A. Basu, Journal of Materials Processing Technology, 77 (1998) 1–3, 17–24
- ⁸ V. Lazić, A. Sedmak, M. Živković, S. Aleksandrović, R. Čukić, R. Jovičić, I. Ivanović, Thermal Science, 14 (2010) 1, 235–246
- ⁹ Y. Wang, H. I. Tsai, Metallurgical and Material Transactions B, 32B (2001) 3, 501–515
- ¹⁰ G. Kosec, F. Vodopivec, A. Smolej, J. V. Tuma, M. Jenko, Mater. Tehnol., 44 (2010) 6, 349–356
- ¹¹ SIST EN 1011-2: 2001, Welding – Recommendations for welding of metallic materials – Part 2: Arc welding of ferritic steels, 2001
- ¹² I. Rak, Tehnologija varjenja, 1. izd., Modrijan, Ljubljana 2008, 312 (in Slovene)
- ¹³ B. Kosec, Metalurgy, 47 (2008) 1, 51–55
- ¹⁴ C. C. Chen, A. Pollack, Influence of welding on steel weldment properties, ASM handbook Welding, Brazing and Soldering, ASM International, reprint 2008, 416–428